# NUCLEAR STRUCTURE STUDIES BY DIRECT REACTIONS WITH RADIOACTIVE BEAMS*

Peter Egelhof

Gesellschaft für Schwerionenforschung (GSI), D-64291 Darmstadt, Germany

*(Received February 1, 1999)*

The investigation of direct reactions with exotic beams in inverse kinematics gives access to a wide field of nuclear structure studies in the region far off stability. The basic concept and the methods involved are briefly discussed. The present contribution will focus on the investigation of light neutron-rich halo nuclei. Such nuclei reveal a new type of nuclear structure, namely an extended neutron distribution surrounding a nuclear core. A brief overview on this phenomenon, and on the various methods which gave first evidence and qualitative confirmation of our present picture of halo nuclei is given. To obtain more quantitative information on the radial shape of halo nuclei elastic proton scattering on neutron-rich light nuclei at intermediate energies was recently investigated for the first time. This method is demonstrated to be an effective means for studying the nuclear matter distributions of such nuclei. The results on the nuclear matter radii of $^6$He and $^8$He, the deduced nuclear matter density distributions, and the significance of the data on the halo structure is discussed. The present data allow also a sensitive test of theoretical model calculations on the structure of neutron-rich helium isotopes. A few examples are presented.

PACS numbers: 21.10.Gv, 25.40.Cm, 25.60.–t, 25.60.Dz

## 1. Introduction

One of the most powerful classical methods for obtaining spectroscopic information on the structure of nuclei is the investigation of light-ion induced direct reactions, *i.e.* elastic or inelastic scattering, or one- and few-nucleon transfer reactions. A lot of what we know about the structure of stable nuclei was obtained from such investigations. Of course, before the availability of radioactive ion beams, this method was limited to stable or very long-lived nuclei, which allow to produce targets. The use of good-quality secondary

* Presented at the XXXIII Zakopane School of Physics, Zakopane, Poland, September 1–9, 1998.

exotic beams now enables to study such reactions on exotic nuclei using the method of inverse kinematics, which is sketched in Fig. 1 for the example of a $(d,p)$ reaction.

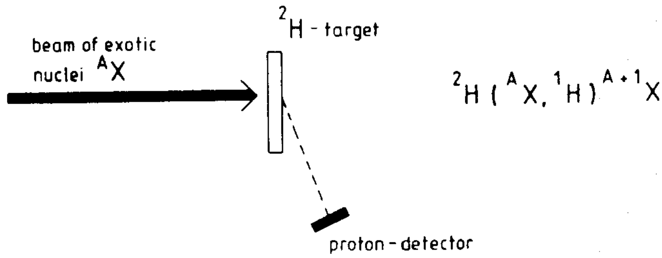


Fig. 1. The method of inverse kinematics is sketched for the example of a $(d,p)$-reaction on the nucleus $^AX$.

In principle, a large variety of light-ion induced reactions with various physics motivations may be investigated. One- and few-nucleon transfer reactions, such as $(d,p)$, $(p,d)$, $(d,t)$, $(d,^3\mathrm{He})$, $(^3\mathrm{He},\alpha)$, *etc.*, allow to populate single-particle (hole) states or two-particle (two-hole) states, whereas inelastic $(p,p')$, $(\alpha,\alpha')$, *etc.* scattering leads to the population of collective states, and $(p,p)$, $(\alpha,\alpha)$, *etc.* elastic scattering allows to deduce information on the nuclear matter distribution of nuclei. Of particular physics interest are, for example, the nuclear shell model in the region far off stability, the two-body residual interaction in nuclei, as well as astrophysical questions, transition densities and deformation parameters, the radial shape of nuclei, *etc.*

The new heavy-ion accelerator facilities at GSI Darmstadt, which came into operation in 1990, opened new opportunities for a variety of nuclear physics studies. With respect to exotic nuclei the combination of the heavy-ion synchrotron SIS, the fragment separator FRS and, for selected cases, the experimental storage ring ESR provides good-quality beams of relatively short-lived nuclei, extending to isotopes far off stability, in the energy range from the Coulomb barrier up to intermediate energies around 1 GeV/u. Especially for experiments with radioactive beams to be performed at intermediate energies the GSI facilities open at present unique possibilities.

The present contribution will focus on nuclear structure studies on light neutron-rich halo nuclei. Such nuclei, located near or at the neutron drip line, in particular $^6$He, $^8$He, $^{11}$Li, $^{14}$Be, *etc.*, have attracted much attention in the recent years since there is clear experimental evidence that these nuclei reveal a qualitatively new type of nuclear structure, namely an extended neutron distribution surrounding a nuclear core.

A brief overview on this phenomenon and on some of the experimental methods which gave first evidence, and which were used for further experimental access to the halo structure of nuclei, is given in the following section. The third section is dedicated to the investigation of nuclear matter distributions of halo nuclei by intermediate energy elastic proton scattering, a method which was applied on exotic nuclei for the first time in recent experiments at GSI.

## 2. Halo nuclei — a new phenomenon of the structure of nuclei

The discovery and the interpretation of the phenomenon of halo nuclei was initiated in the mid-eighties by the pioneering work of Tanihata and coworkers [1–3]. In these experiments the total interaction cross section $\sigma_I$ was determined for the interaction of light neutron-rich isotopes with various targets. $\sigma_I$ was deduced from the change of intensity of a beam of exotic nuclei before and after hitting a target. From the measured interaction cross sections the nuclear matter radii $R_I$ (proj.) of the projectile nuclei may be estimated by simple geometrical considerations using the relation

$$\sigma_I = \pi[R_I(\text{proj.}) + R_I(\text{tar.})]^2, \tag{1}$$

$R_I(\text{tar.})$ being the matter radius of the target nucleus. (It should be noted that for a quantitative determination of the matter radii a more sophisticated analysis taking into account the reaction dynamics was used.)
The surprisingly steep rise of $\sigma_I$ for $^{11}$Li in the chain of the Li-isotopes, and less pronounced, for $^{6}$He and $^{8}$He for the He-isotopes, was therefore interpreted as due to a pronounced increase of the nuclear matter radius. In Fig. 2 a compilation of such data [3] measured for a larger number of neutron-rich isotopes is displayed. In almost all of the isotope chains we observe for the most neutron-rich nuclei a deviation from the A$^{(1/3)}$-law (see dotted line in Fig. 2), which is well established for stable and less exotic nuclei. These findings were at that time interpreted in terms of the following picture (see also Fig. 3): For the case of "normal" nuclei, which are stable or are situated close to the valley of stability, and which therefore possess only a small excess of neutrons, the neutrons and protons are equally distributed (left part of Fig. 3), and the addition of one neutron will not drastically change the spatial extension of the nucleus. In contrast, a new phenomenon of nuclear structure appears for some nuclei which are close to the drip line, and for which the binding energy of additional valence nuclei is consequently very low, usually of the order of a few hundred keV only. Adding one or more neutrons to such an already very neutron-rich nucleus will produce in certain cases a so-called "halo" around a nuclear core, consisting of an extremely spatially extended, low-density aureole in which the additional neutrons are located (right part of Fig. 3). Thus, in special cases, a significant fraction of more than 90% of the valence neutron wave function can be outside of

the central part of the nucleus, leading to an extended radius of the nuclear matter distribution. So, for example, the nuclear radius determined for $^{11}$Li is similar to that of the stable $^{32}$S, which consists of approximately three times the number of nucleons. It turns out that the phenomenon of halo nuclei is always closely connected to a very low binding energy of the valence nucleons.

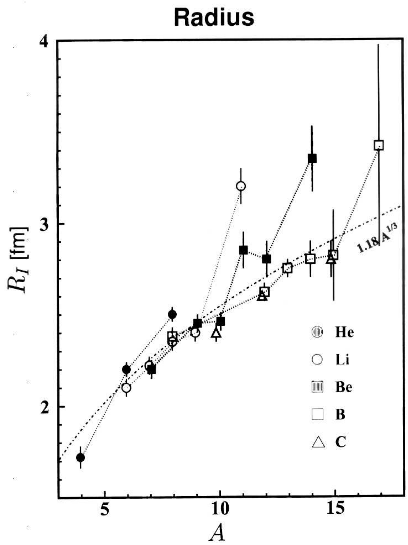


Fig. 2. Nuclear matter radii $R_I$ deduced from measured total interaction cross sections for several isotope chains of light neutron-rich nuclei (from Ref. [3]).

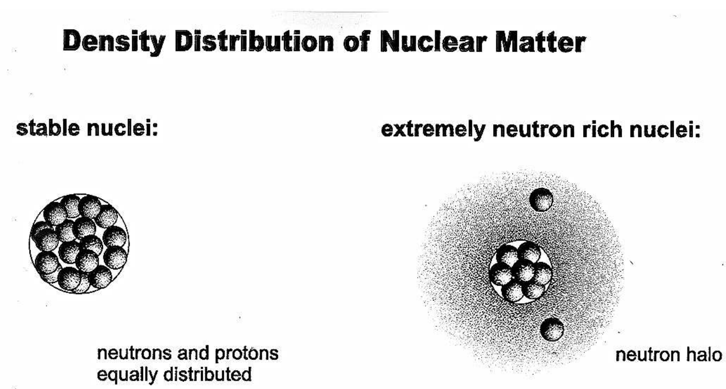


Fig. 3. Density distributions of nuclear matter for stable nuclei and extremely neutron-rich nuclei.

In order to confirm the present picture of halo nuclei, and to get a deeper insight into the structure of such nuclei, halo nuclei were subject to numerous studies during the last decade, using various methods. For a detailed overview over this field the reader may be referred to recent review articles [4–7]. Experiments performed at the on-line mass separator ISOLDE at CERN focused on the electric and magnetic moments of halo nuclei [8, 9]. Beta-decay measurements following in-beam polarization by optical pumping on $^{9}$Li and $^{11}$Li showed that the electric and magnetic properties of both nuclei are very similar. This finding is a clear confirmation that the large interaction cross section obtained for $^{11}$Li is only due to the spatial distribution of the valence neutrons, and not created by core deformation or core polarization effects.

Another frequently used method is the investigation of momentum distributions of the reaction products after fragmentation of the halo nucleus following the interaction with a target. Experiments were performed using beams produced by heavy ion projectile fragmentation and in-flight separation at GANIL, MSU, RIKEN in the energy range 20–80 MeV/u, and at BEVALAC and GSI for higher incident energies of about 200–1000 MeV/u. Thus, a large variety of data on longitudinal and transverse momentum distributions of the heavy "core"-fragment, and of the valence neutrons, and, in kinematical complete experiments, of both have been taken for various exotic nuclei, and for various targets and incident energies (for an overview see [4–7, 10], and references therein).

It follows from relatively simple considerations that the momentum distributions of the fragments reflect the intrinsic distribution of the constituents, and thus the spatial structure of the fragmenting nucleus. The momentum distribution of the valence neutrons of the nucleus being the Fourier transform of its wave function, the size of the spatial distribution of the nucleus is — due to the uncertainty principle — expected to be inversely proportional to the width $\Gamma$ of the momentum distribution. Hence we obtain for the root mean square matter radius:

$$\langle R_{\mathrm{m}}^2 \rangle^{1/2} \sim 1/\Gamma \,. \tag{2}$$

Indeed, narrow momentum distributions were obtained for practically all candidates for halo nuclei, as established from the data on the total interaction cross section. As an example, recent data [11] on longitudinal momentum distributions of $^{18}$C ($^{16}$C)-fragments after one-neutron removal from $^{19}$C ($^{17}$C)-projectiles are displayed in Fig. 4. Both projectile nuclei are assumed to have an extended neutron distribution due to the small binding energy of the valence neutron. Consequently both momentum distributions are found to be narrower by factors of about 2 and 3 compared to the corresponding momentum distributions of tightly bound nuclei, thus confirming an extended neutron distribution in both nuclei. The significant difference in the width of the distributions is attributed to the difference in the separation energies of the valence neutron, and thus a pronounced halo structure is established for the $^{19}$C nucleus. Fig. 5 displays the latest compilation of nuclei for which the halo structure has been confirmed by the various experimental information. Besides one-, two-, and four-neutron halos on the neutron-rich side, there is meanwhile also evidence for proton halos.

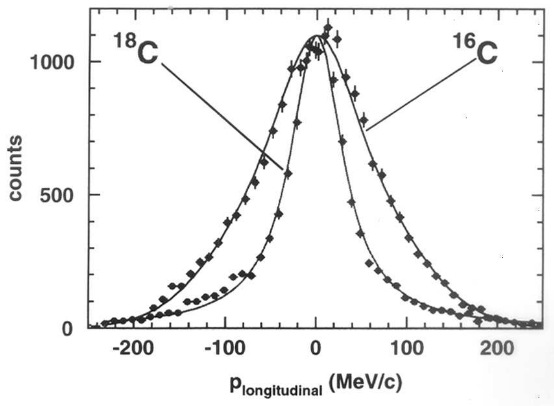


Fig. 4. Longitudinal momentum distributions of $^{18}$C, and $^{16}$C after one-neutron removal from $^{19}$C, and $^{17}$C, respectively (from Ref. [11]).

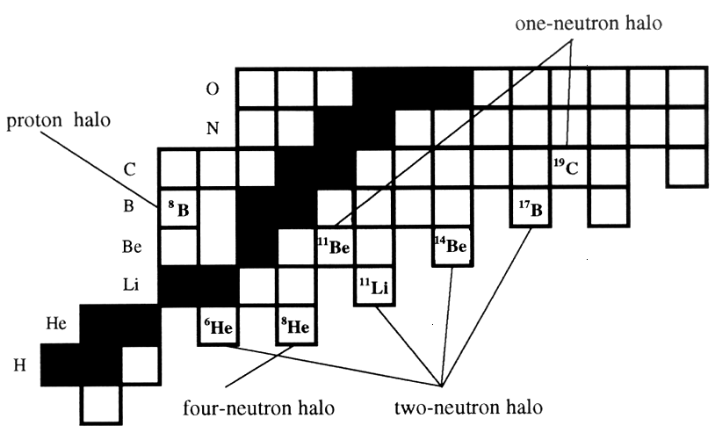


Fig. 5. Chart of isotopes up to element $Z = 8$. Nuclei for which a halo structure was confirmed experimentally are indicated.

In summary we conclude that the assumed picture on the structure of halo nuclei, established after the finding of the large interaction radii (see above), was qualitatively confirmed by various experiments. Halo nuclei are thus characterized by large interaction cross sections, weak binding of the valence nucleon(s), and narrow momentum distributions of the reaction products after fragmentation. On the other hand it should be pointed out, that a more quantitative information on the radial structure and the size of halo nuclei from such experiments is to a considerable extend limited by the limited knowledge of the underlying reaction mechanism and dynamics of the reactions used. Hence, systematic uncertainties in the determination of the matter radii appear due to uncertainties created by effects like the interaction of the target with the nuclear constituents, by the final state interaction of the knocked-out fragments with the remaining system, *etc.* Thus, in order to obtain more quantitative information on the radial shape of halo nuclei and the nuclear matter radii, the method of elastic proton scattering at intermediate energy was recently applied, as will be discussed in the following Section.

## 3. Nuclear matter distributions of halo nuclei from elastic proton scattering at intermediate energy

Proton nucleus elastic scattering at intermediate energies was proved (for the case of stable nuclei) to be a well suited method for obtaining accurate and detailed information on nuclear matter distributions of nuclei [12]. This method was recently applied at GSI Darmstadt for the first time for the investigation of exotic nuclei. The advantage of such experiments as compared to investigations at considerably lower incident energies is, that for intermediate energies, available for exotic beams at GSI, proton-nucleus elastic scattering can be described accurately by the diffractive multiple scattering theory which relates the measured cross section to the nuclear matter distribution in a rather unambiguous way [12]. Furthermore, as theoretical considerations have shown [13, 14], proton scattering in the region of small momentum transfer is sensitive to the halo structure of nuclei. Thus, besides the precise determination of the nuclear matter radius, information on the shape of the radial distribution of nuclear matter of halo nuclei can be obtained. Both quantities are fundamental quantities of nuclei, and therefore of large interest for our understanding of the structure of halo nuclei, and for an effective test of respective theoretical model calculations.

Differential cross sections for elastic proton scattering at small scattering angles were measured at GSI Darmstadt at energies around 700 MeV/u in inverse kinematics for the neutron-rich helium isotopes $^{6}$He, $^{8}$He [15,16], and recently also for the neutron-rich lithium isotopes $^{8}$Li, $^{9}$Li, and $^{11}$Li. The present contribution will mainly concentrate on data on the helium isotopes for which the data analysis was completed recently [14]. Secondary $^{4,6,8}$He beams (the $p^4$He cross section was measured for a consistency check of the method) were produced with incident energies of 699 MeV/u, 717 MeV/u, and 674 MeV/u, respectively, by fragmentation of $^{18}$O ions from the heavy-ion synchrotron SIS, impinging on a beryllium target, and were isotopically separated by the fragment separator FRS [17]. The intensity of the secondary beams was about $10^3$ sec$^{-1}$ in all cases.

The experimental setup is displayed in Fig. 6 (for more details on the technical design and experimental procedure see also Refs. [16, 18]). The relatively low secondary beam intensities for isotopes close to the drip line demand for a thick effective hydrogen target, and for a large solid angle detector for the recoil protons. In order to meet these experimental conditions the hydrogen filled time-projection ionization chamber IKAR was used, which serves simultaneously as a gas target and a detector. It was developed at the St. Petersburg Nuclear Physics Institute (PNPI), Gatchina, and was originally used for studying small angle hadron elastic scattering [19]. IKAR ensures a high $H_2$ target thickness (about $3\times10^{22}$ protons/cm$^2$), and has a $2\pi$ acceptance in azimuthal angle for recoil proton registration. It operates at 10 bar pressure of hydrogen and consists of 6 identical modules. Each module contains an anode plate, a cathode plate, and a grid, all electrodes being arranged perpendicular to the beam direction. The signals from the electrodes, registered by flash analog-to-digital converters, provide the energy of the recoil proton, or its energy loss in case it leaves the active volume, the scattering angle of the recoil proton, and the coordinate of the interaction point in the grid-cathode space. The scattering angle for the helium projectiles was determined by a tracking detector consisting of 4 two-dimensional multiwire-proportional chambers (see Fig. 6). In addition, the scintillation counters S1, S2, S3, and VETO were used for triggering, and for the identification of the incident and scattered beam particles via time-of-flight and $dE/dx$ measurements.

The resulting cross sections are displayed in Fig. 7. Plotted error bars denote statistical errors only. The absolute normalization obtained is estimated to be accurate within $\pm$ 3%. The measured $p^4$He cross section is in excellent agreement with previous data [20], which were obtained in direct kinematics.

To derive information on the nuclear density distributions of $^6$He and $^8$He from the measured cross sections the Glauber multiple scattering theory was applied. Calculations were performed using the basic Glauber formula [12] for proton-nucleus elastic scattering, and taking experimental data on proton-proton and proton-neutron scattering as an input. For the analysis of the present experiment [14, 15] various parametrizations of the nuclear

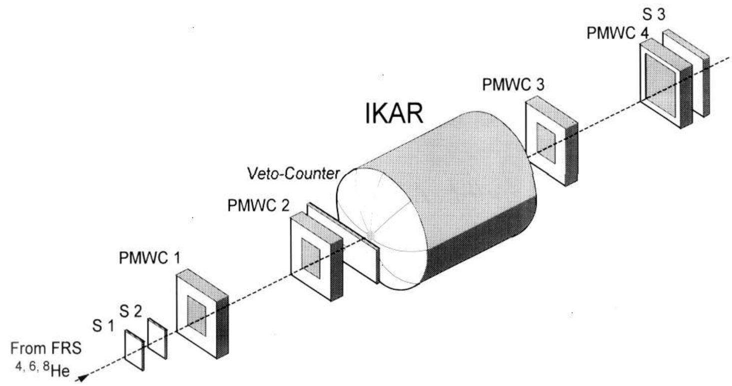


Fig. 6. Schematic view of the experimental setup. The central part shows the hydrogen filled ionization chamber IKAR which serves simultaneously as a gas target and a detector system for recoil protons. Four multiwire proportional chambers (PMWC 1-4) determine the scattering angle of the projectile. Scintillation counters (S1-S3, VETO) were used for trigger and particle identification.

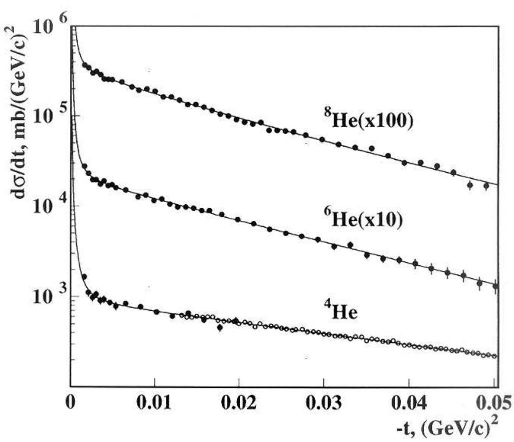


Fig. 7. Absolute differential cross sections $d\sigma/dt$ versus the four momentum transfer squared $-t$ for $p^4$He,$p^6$He and$p^8$He elastic scattering at incident energies of 699 MeV/u, 717 MeV/u, and 674 MeV/u, respectively, obtained from the present experiment (full dots). Open dots show the data of Ref. [20]. Full lines are the result of fits assuming the GH parametrization for the nuclear density distributions.

density distributions of $^4$He, $^6$He and $^8$He were used as an input for the Glauber calculations, and the parameters were varied in order to obtain a best fit to the experimental cross sections. All nucleon distributions deduced, as well as the resulting root mean square radii $R_{\rm m}$, refer to point nucleon distributions. Two parametrizations of the total matter distribution $\rho_m(r)$ were used which do not make a difference between core and valence nucleons, namely a symmetrized Fermi (SF) distribution, and a Gaussian with a "halo" (GH) (for details see Ref. [14]). Furthermore two parametrizations were applied which assume that the $^{6,8}$He nuclei consist of an $\alpha$ core and of 2(4) valence neutrons for $^6$He ($^8$He). Here, a Gaussian distribution for the core, and either a Gaussian (GG) or a $1p$-shell harmonic oscillator-type density (GO) for the valence neutrons were used.

The experimental data are equally well described independent on the density parametrization used, with a reduced $\chi^2$ around unity. Solid lines in Fig. 7 show the GH case as an example. The deduced nuclear matter density distributions $\rho_m(r)$ for $^6$He and $^8$He are displayed in Fig. 8 in comparison with the one for $^4$He. The results for all four parametrizations used agree reasonably well, within small errors (for a detailed discussion see Ref. [14]) over a wide range of the radius parameter $r$. For both neutron-rich He isotopes, $^6$He and $^8$He, rather extended matter distributions were obtained, the matter densities decreasing much slower with the radius than the one for $^4$He. This result is interpreted as a clear evidence for the existence of a significant neutron halo in $^6$He and $^8$He.

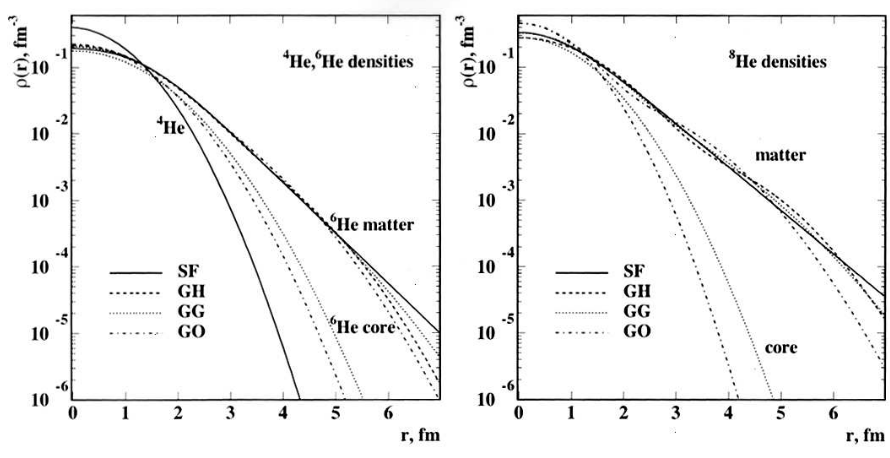


Fig. 8. Nuclear core and nuclear matter density distributions $\rho$(r) for $^6$He (left side) and for $^8$He (right side) obtained for the different parametrizations applied (for notations see text). For a comparison the nuclear matter density distribution for $^4$He is also plotted (left side). Curves are normalized to the number of nucleons.

Both parametrizations (SF and GH) applied for $^4$He have yielded identical values $R_{\rm m} = 1.49 \pm 0.03$ fm. In the case of $^6$He and $^8$He the values obtained for the matter radii $R_\mathrm{m}$ from the four parametrizations mutually agree within small errors ($\pm 0.02$ fm). This demonstrates that the results on the radii are quite independent on the model assumptions considered. The final average values are $R_\mathrm{m} = 2.30 \pm 0.07$ fm for $^6$He, and $R_\mathrm{m} = 2.45 \pm 0.07$ fm for $^8$He (with total errors including systematical uncertainties).

The present data on nuclear matter radii from elastic proton scattering cross sections may be compared to corresponding data deduced from the total interaction cross sections, a method which was discussed in section 2 of this contribution. Such a comparison is of special interest, as both methods to determine nuclear matter radii are independent.

The results from the present experiment are in close agreement with the for years accepted values $R_\mathrm{m} = 2.33 \pm 0.04$ fm for $^6$He and $R_\mathrm{m} = 2.49 \pm 0.04$ fm for $^8$He from Tanihata *et al.* [23]. However, the data on the $^6$He matter radius from the total interaction cross sections were again under discussion recently, as a reanalysis [24, 25] of the data from Ref. [2] resulted in two new values for $R_\mathrm{m}$, which both disagree with the radius from the present experiment. In Fig. 9 the results on the matter radius of $^6$He from various analysis [21–25] over the years, which were all based on the same experimental data set from Tanihata *et al.* [2], are displayed (black dots). For comparison the result of the present experiment is also shown in Fig. 9 (open square). It may be concluded from Fig. 9 that the error bars given for the various values deduced from analysing the data on the total interaction cross section do in some cases not include, or underestimate the systematical uncertainties. At present this topic is still under discussion.

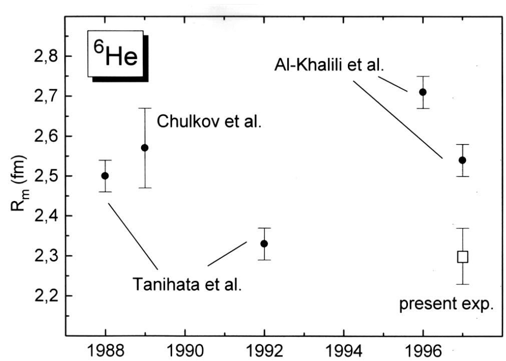


Fig. 9. Compilation of values for the nuclear matter radius of $^6$He, deduced from various analysis [21–25], which were all based on the same data set on the total interaction cross sections [2] (black dots). For comparison the value obtained from the present experiment is also shown (open square).

Besides the determination of phenomenological nucleon density distributions and their parameters, the present data allow also a sensitive test of theoretical model calculations on the structure of neutron-rich nuclei. As an example, the results of microscopic calculations performed in the framework of the Refined Resonating Group Model (RRGM) [26], using as an input various effective nucleon–nucleon forces without additional free parameters, are compared with the experimental data. For that purpose, the nucleon density distributions obtained from the theoretical RRGM calculations [27, 28] for the different helium isotopes investigated were used as an input for Glauber calculations, as described above. Finally the obtained "theoretical cross sections" were compared with the experimental data, thus allowing for a test of the nucleon–nucleon force used. In Fig. 10 the experimental data on $^6$He and $^8$He are displayed in comparison with the corresponding results of RRGM calculations [27, 28] performed with the effective nucleon–nucleon force introduced by Csoto (CS), and various modifications of the effective nucleon–nucleon force introduced by Stöwe and Zahn (SZ) (for details see Refs. [18, 27, 28]). For both isotopes, the SZ-V2 force, which includes (as compared to the original version SZ-2) the central force in the odd-parity singlet and triplet states of the nucleon–nucleon two-body force, yields the best description of the experimental data. In the case of $^8$He the SZ-V2

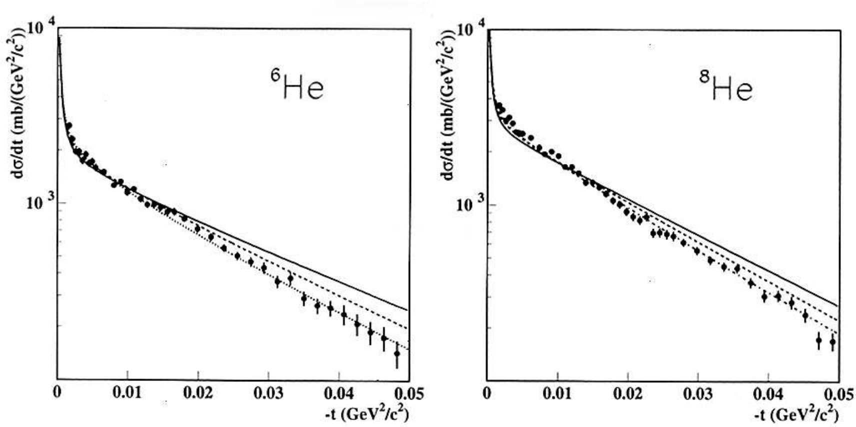


Fig. 10. Differential cross sections for $p^6$He scattering (left side) and $p^8$He scattering (right side) obtained from the present experiment are compared with calculated cross sections on the basis of nuclear matter distributions resulting from microscopic RRGM calculations with various effective nucleon–nucleon forces, namely CS (solid lines), SZ (dashed lines), SZ-V2 (dotted line), modified SZ-V2 (dashed-dotted line). For notations see text.

force had to be modified [28] (inclusion of a realistic hard core) to obtain a reasonable agreement with the experimental data.

In Fig. 11 (left side) the corresponding theoretical nuclear matter density distributions are, for the case of $^6$He, compared with the distribution deduced from the present experiment for the GG parametrization (see above). For $r < 5$ fm, the best agreement is obtained for the SZ-V2 force which gave also the best agreement for the cross sections. There seems to be a general trend of these calculations to exhibit, as compared to the experimental result, an enhanced tail for very large radii ($r > 5$ fm). This trend is in agreement with calculations from Ref. [24], but in disagreement with a recent calculation using the boson dynamic-correlation model [29]. The result of this calculation is also shown in Fig. 11 (right side). A remarkably good agreement with the experimentally determined density distribution over the whole range of the radius parameter $r$ is obtained.

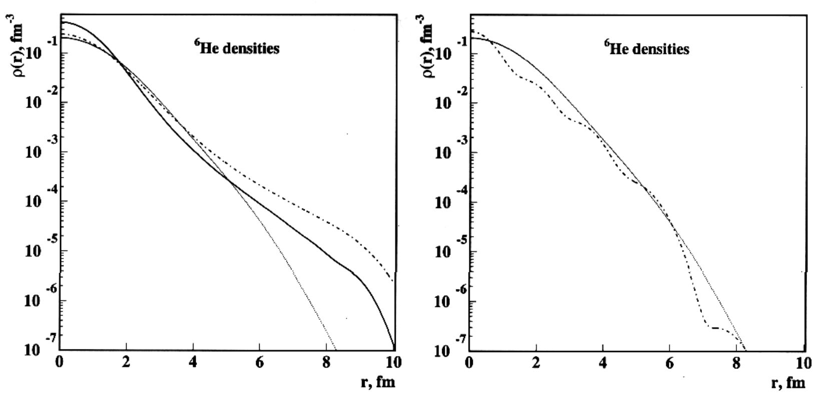


Fig. 11. On the left side the nuclear matter density distribution for $^6$He obtained from microscopic RRGM calculations with the effective nucleon–nucleon forces CS (solid line) and SZ-V2 (dashed- dotted line) are compared with the density distribution deduced from the present experiment for the GG parametrization (dotted line). On the right side of the figure, again the distribution deduced from the present experiment (dotted line) is compared with the result of a calculation using the boson dynamic-correlation model [29] (dashed-dotted line).

In an experiment performed very recently at GSI Darmstadt data on elastic proton scattering from neutron-rich lithium isotopes $^8$Li, $^9$Li and $^{11}$Li were taken using the same experimental method. At present the data analysis is in progress. From the statistics obtained we expect a similar, or even better sensitivity on the nuclear matter distributions of $^{8,9,11}$Li as compared to the case of the helium isotopes.

The author is indebted to G.D. Alkhazov, H.M. Hofmann, M. Mutterer, and S.R. Neumaier for many stimulating discussions, and to M. Mutterer and S.R. Neumaier for a critical reading and for the help in preparing the manuscript.

## REFERENCES

[1] I. Tanihata *et al.*, *Phys. Rev. Lett.* **55**, 2676 (1985).
[2] I. Tanihata *et al.*, *Phys. Lett.* **B160**, 380 (1985).
[3] I. Tanihata, *Nucl. Phys.* **A488**, 113c (1988).
[4] K. Riisager, *Rev. Mod. Phys.* **66**, 1105 (1994).
[5] P.G. Hansen *et al.*, *Ann. Rev. Nucl. Part. Sci.* **45**, 591 (1995).
[6] I. Tanihata, *Prog. Part. Nucl. Phys.* **35**, 505 (1995).
[7] I. Tanihata, *J. Phys.* **G22**, 157 (1996).
[8] E. Arnold *et al.*,*Phys. Lett.* **B197**, 311 (1987).
[9] E. Arnold *et al.*,*Phys. Lett.* **B281**, 16 (1992).
[10] H. Emling, *J. Phys.* **G24**, 1561 (1998).
[11] T. Baumann *et al.*, *Phys. Lett.* **B439**, 256 (1998).
[12] G.D. Alkhazov *et al.*, *Phys. Rep.* **C42**, 89 (1978).
[13] G.D. Alkhazov *et al.*, *Pisma ZhETF* **55**, 377 (1992); *JETP Lett.* **55**, 379 (1992).
[14] G.D. Alkhazov *et al.*, *Nucl. Phys.* A (1999), to be published.
[15] G.D. Alkhazov *et al.*, *Phys. Rev. Lett.* **78**, 2313 (1997).
[16] S.R. Neumaier *et al.*, *Nucl. Phys.* **A** (1999), to be published.
[17] H. Geissel *et al.*, *Nucl. Instr. Meth.* **B70**, 286 (1992).
[18] S.R. Neumaier *et al.*, *Proc. Int. Conf. on Exotic Nuclei and Atomic Masses*, ENAM, Arles, France, Edit. Front., 1995, p.227.
[19] A.A. Vorobyov *et al.*, *Nucl. Instr. Meth.* **119**, 509 (1974).
[20] O.G. Grebenjuk *et al.*, *Nucl. Phys.* **A500**, 637 (1989).
[21] I.Tanihata *et al.*, *Phys. Lett.* **B206**, 592 (1988).
[22] L. V. Chulkov *et al.*, *Europhys. Lett.* **8**, 245 (1989).
[23] I.Tanihata *et al.*, *Phys. Lett.* **B289**, 261 (1992).
[24] J. S. Al-Khalili *et al.*, *Phys. Rev.* **C54**, 1843 (1996).
[25] J. S. Al-Khalili *et al.*, *Nucl. Phys.* **A616**, 418c (1997).
[26] H.M. Hofmann, *Lecture Notes in Physics* **273**, 243 (1987).
[27] J. Wurzer *et al.*, *Phys. Rev.* **C55**, 688 (1997), and references therein.
[28] J. Wurzer, PhD thesis, University of Erlangen, 1997.
[29] M. Tomaselli *et al.* (1999), to be published.